

## ENERGY TRANSFORMATION DURING THE PIERCE PROCESS IN THE PRODUCTION OF SEAMLESS PIPES

Ladislav Lazić<sup>1)\*</sup>, Martina Lovrenić - Jugović<sup>1)</sup>, Željko Grubišić<sup>1)</sup>

<sup>1)</sup> University of Zagreb, Faculty of Metallurgy, Sisak, Croatia

Received: 05.02.2016

Accepted: 03.02.2016

\*Corresponding author: *e-mail: lazic@simet.hr, Tel.: +385 44 533 378, Department of Mechanical Metallurgy, Faculty of Metallurgy, University of Zagreb, Aleja narodnih heroja 3, 44103 Sisak, Croatia*

### Abstract

In the line for production of seamless pipes the pierce and pilger method, also known as the Mannesmann process, are used for the production of seamless tubes. Following the cross roll piercing operation, the tick-walled hollow shell is rolled out in the same internal energy in the pilgering stand, in which the tick-walled hollow shell is elongated to the finished tube dimensions by the discontinuous forging action of the pilger rolls on a mandrel located inside the hollow shell. On the basis of the measured essential parameters, the formulated mathematical model for energy transformations during the piercing process was validated. The model allows the calculation of temperature increment of the rounds depending on the temperature rounds before piercing and consumed electricity of electric motor for drive of the stand rolls.

**Keywords:** metal forming, piercing process, energy transformation

### 1 Introduction

Steel and iron making industries have been driven by the requirements of maintaining or improving product quality and minimization of production costs. Within these requirements the overall energy management and energy efficiency play important roles [1-4].

Energy efficiency of a reheating furnace for stock heating prior to hot forming depends on various parameters of the heating process [5-8]. The greatest influence on the furnace energy efficiency has the temperature of the heated stock at the outlet of the furnace, and in connection therewith the set furnace temperature regime. The stock heating is being realized in the rotary hearth furnace in the line for seamless pipe production, of the nominal heating capacity of 27 t/h. Heated material has the following features: roundshape of 280÷410 mm, length of 600÷2600 mm, mass of 300÷1750 kg, steel quality - St 37, St 35, St 52 etc. Passing through various temperature zones in a natural gas fired rotary hearth furnace, the round cast stock is heated to rolling temperature, which depends on the material composition but generally in the range from 1260 to 1280°C.

In the line for production of seamless pipes the pierce and pilger method, also known as the Mannesmann process, are used for the production of seamless tubes. The piercing mill consists of two special countered work rolls which are driven in the same direction of rotation. Their axes are inclined by approx. 3 to 6° in relation to the horizontal stock plane. Generally, the roll gap is closed by a non-driven support roll at the top and a support shoe at the bottom.

**Fig. 1** shows a schematic representation of the sequence of cross roll piercing process [9]. The round is thrust into the mill, gripped by the tapered inlet section of the rolls to be formed in a

spiral motion over the piercing mandrel to produce the tick-walled hollow shell. Once the mandrel engages in the newly formed mouth of the worked round, the material is continuously deformed as it passes between the rolls and over the mandrel. **Fig. 2** shows a piercing mill in the line for seamless tubes production.

Following the cross roll piercing operation, the tick-walled hollow shell is rolled out in the same internal energy in the pilgering stand, in which the tick-walled hollow shell is elongated to the finished tube dimensions by the discontinuous forging action of the pilger rolls on a mandrel located inside the hollow shell [9].

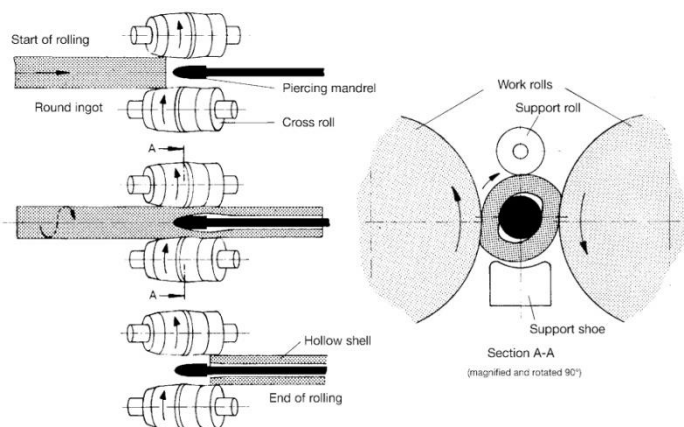


**Fig. 1** Schematic representation of the sequence of cross roll piercing process [9]



**Fig. 2** The photographs of piercing mill in the line for seamless tubes production

Numerous experimental and analytical studies and the computer programs that can analyze the deformation and temperature of a material during roll piercing processes in seamless pipe production have been performed [10-15]. This paper aims to formulate a mathematical model for energy transformations during the piercing process, i.e. to determine computationally the temperature increase of the tick-walled hollow shell after the cross roll piercing operation. The first step is to formulate a mathematical model, and then to carry out validation procedure of the model with measurement results.

## 2 The structure of the formulated calculation model

Calculation model of temperature increment depending upon the amount of used mechanical energy is based on the calculation method described in Ref. [16].

The total heat flow ( $\Phi$ ) being absorbed by a round during cross roll piercing operation, as a result of the transformation of mechanical energy for drive of the work rolls to internal energy of rolled round, is:

$$\Phi = m \cdot c_p \cdot (\vartheta_{in} - \vartheta_{out}) / t \quad , \quad \text{W} \quad (1)$$

where are:  $m$  - mass of the round , kg  
 $c_p$  - specific heat capacity of the round, J/(kg·K)  
 $\vartheta_{in}$  - inlet temperature of the round, °C  
 $\vartheta_{out}$  - outlet temperature of the round, °C  
 $t$  - deformation time, s

Transformed mechanical energy to internal energy of the rolled round, discounting the energy loss by friction and heat transfer by convection and radiation on the environment, is:

$$\Phi = P \cdot \eta \quad , \quad (2)$$

where are:  $P$  - electromotor power during the cross roll piercing operation (discounting the energy loss by friction and heat transfer by convection and radiation on the environment), W  
 $\eta$  - piercing mill efficiency.

Considering that  $\eta=1$  and with combination of above two expressions, the equation for calculation of the temperature increase of the tick-walled hollow shell is obtained in the next form:

$$\vartheta_{out} - \vartheta_{in} = \frac{t}{m \cdot c_p} \cdot P \quad , \quad ^\circ\text{C} \quad (3)$$

Taking into account the energy loss by convection and radiation from the rolled piece on the environment, the next energy balance in the differential form may be set for the cross roll piercing operation:

$$\Phi \cdot dt = \rho \cdot V \cdot c_p \cdot d\vartheta + \alpha \cdot A \cdot (\vartheta - \vartheta_{\infty}) \cdot d\vartheta \quad , \quad (4)$$

where are:  $\rho$  - density of material, kg/m<sup>3</sup>  
 $V$  - volume of rolled piece , m<sup>3</sup>  
 $A$  - outer surface of rolled piece , m<sup>2</sup>  
 $\alpha$  - total coefficient of heat transfer, W/(m<sup>2</sup>·K)  
 $\vartheta_{\infty}$  - temperature of environmental air, °C

With the increase of temperature the density generally decreases according to the following expression:

$$\rho_{\vartheta} = \frac{\rho_{20}}{1 + 3 \cdot \beta \cdot (\vartheta - 20)} \quad \text{kg/m}^3 \quad , \quad (5)$$

where are:  $\rho_g$  - density of material at  $g$ ,  $\text{kg/m}^3$   
 $\rho_{20}$  - density of material at  $g = 20^\circ\text{C}$ ,  $\text{kg/m}^3$   
 $\beta$  - linear coefficient of expansion of the round material,  $1/\text{K}$ .

The solution of differential equation (4) may be presented in the next forms [4]:

$$g_{\text{out}} = g_{\infty} + \frac{\Phi}{\alpha \cdot A} \cdot \left( 1 - e^{-\frac{\alpha \cdot A \cdot t}{c_p \cdot \rho \cdot V}} \right) + (g_{\text{in}} - g_{\infty}) \cdot e^{-\frac{\alpha \cdot A \cdot t}{c_p \cdot \rho \cdot V}}, \quad (6)$$

$$\frac{g_{\text{out}} - g_{\infty}}{g_{\text{in}} - g_{\infty}} = \frac{\Phi}{\alpha \cdot A \cdot (g_{\text{in}} - g_{\infty})} \cdot \left( 1 - e^{-\frac{\alpha \cdot A \cdot t}{c_p \cdot \rho \cdot V}} \right) + e^{-\frac{\alpha \cdot A \cdot t}{c_p \cdot \rho \cdot V}}. \quad (7)$$

Taking into account the ratio of the mass  $m$  and surface  $A$  of the body, the factor  $K_1$  may be introduced in calculation in the following way:

$$\frac{m}{A} = \frac{\rho \cdot V}{A} = \frac{\rho \cdot S}{K_1} \quad (8)$$

where are:  $K_1$  - factor which depends on the shape of the body (for cylinder  $K_1 = 2$ )  
 $S$  - calculation thickness or characteristic dimension of the body (for cylinder  $S = r$ ), m

The heat flow from the body to the environment with respect to the initial temperature of the body:

$$\Phi_0 = \alpha \cdot A \cdot (g - g_{\infty}). \quad (9)$$

In the calculation is necessary to define whether it is massive or thin body according to the value of the Biot number ( $Bi$ )

$$Bi = \frac{\alpha \cdot S}{\lambda}. \quad (10)$$

Bodies can be assumed to be thin at  $Bi \leq 0.25$ , massive at  $Bi \leq 0.5$  and  $0.25 < Bi < 0.5$  is transitional area in which bodies can be referred to one or the other class depending on the desired accuracy of calculation [17]. Introducing the factor of massiveness of the body ( $\psi$ ), which is determined based on the Biot number [16]:

$$\psi \cong \frac{1}{1 + \frac{Bi}{K_1 + 2}} \quad \text{for } Bi \leq 4, \quad (11)$$

and substituting equations (8), (9) and (11) into (7), the following equation is obtained:

$$\frac{g_{\text{out}} - g_{\infty}}{g_{\text{in}} - g_{\infty}} = \frac{\Phi}{\Phi_0} \cdot \left( 1 - e^{-\frac{K_1 \cdot \psi}{\rho \cdot S} \cdot \frac{\alpha \cdot t}{c_p}} \right) + e^{-\frac{K_1 \cdot \psi}{\rho \cdot S} \cdot \frac{\alpha \cdot t}{c_p}}. \quad (12)$$

Introducing the Biot (10) and Fourier number ( $F_0$ ) as well as the coefficient of thermal diffusivity ( $a$ ),

$$Fo = \frac{a \cdot t}{S^2}, \quad a = \frac{\lambda}{c_p \cdot \rho}, \quad (13)$$

and taking into account the equality of  $Fo \cdot Bi = \frac{a \cdot t}{S^2} \cdot \frac{\alpha \cdot S}{\lambda} = \frac{1}{\rho \cdot S} \cdot \frac{\alpha \cdot t}{c_p}$ , the expression (12) can be written as:

$$\frac{\vartheta_{\text{out}} - \vartheta_{\infty}}{\vartheta_{\text{in}} - \vartheta_{\infty}} = \frac{\Phi}{\Phi_0} \cdot \left(1 - e^{-K_1 \cdot \psi \cdot Fo \cdot Bi}\right) + e^{-K_1 \cdot \psi \cdot Fo \cdot Bi}. \quad (14)$$

The expression (14) was used in the calculation model.

### 3 Measurement and calculation results

The quality of round conticast was Č8380 (API N-80) (0.28-0.34% C, ≤0.4% Si, 1.1-1.4% Mn, ≤0.035% P, ≤0.035% S, 0.16-0.22% V). **Fig. 3** shows a diagram of the recorded changes of the basic indicators of work of the electric motor during cross roll piercing operation. The red curve shows the current strength of the electric motor and the blue curve the number of revolutions of rolls.

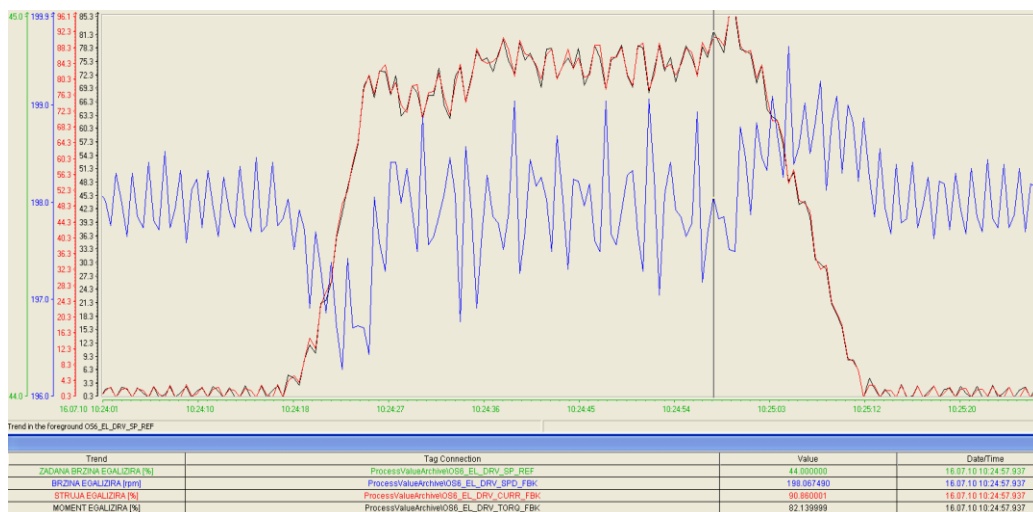


**Fig. 3** Changing the current strength and the number of revolutions of the electric motor during cross roll piercing operation

**Table 1** shows the input data in the calculation of the increase of temperature. The averaged value of the current strength is determined based on the diagram in **Fig. 3**. The values of averaged power ( $P$ ) and the consumed electricity ( $E$ ) are shown in **Table 1**.

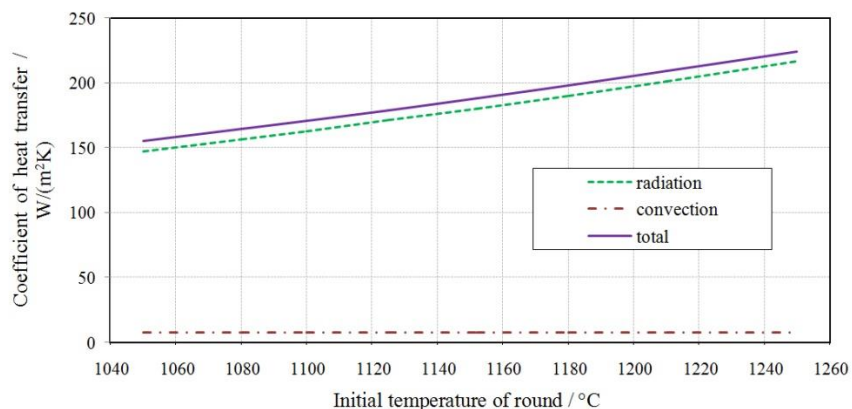
According to the methodology of calculation of heat transfer by convection described in Ref. [18], the overall heat transfer coefficient from the round on the environment depending on the initial temperature of round is calculated (**Fig. 3**).

**Table 1** Input data

Parameter	Value	Unit	Description
$\vartheta_{in}$	1080	°C	inlet temperature of the round
$\vartheta_{\infty}$	27	°C	temperature of environmental air
$d$	0.28	m	diameter of the round
$l$	1.35	m	length of the round
$S$	0.14	m	characteristic dimension
$U$	850	V	supply voltage
$\eta$	0.937	-	efficiency of the electric motor
$t$	54	s	time of cross roll piercing operation
$I$	1 513.974	A	averaged value of current strength
$P = U \cdot I$	1 286.878	kW	averaged power
$E = P \cdot t$	20.436	kWh	consumed electricity

**Table 2** Material properties of rounds in a function of temperature

Parameter	Value	Unit	Description
$\lambda$	29	W/(m·K)	thermal conductivity of the round
$c_p$	712	J/(kg·K)	specific heat capacity of the round
$\beta$	$13.7 \cdot 10^{-6}$	1/K	linear coefficient of expansion of the round
$\varepsilon$	0.87	-	emissivity of the round

**Fig. 4** Overall heat transfer coefficient from the round on the environment depending on the initial temperature of round

The calculation results are shown in **Table 3**.

In order to validate the above described model, the calculated values of temperature increase of the tick-walled hollow shells for different inlet temperatures of the rounds ( $\vartheta_{in,exp}$ ) were compared with the measured values. The diagram in **Fig. 5** shows the measured data of averaged motor power ( $P_{exp}$ ) depending on the initial temperature of the rounds. By method of least squares the interpolation curve is obtained. For the same initial temperatures, using the model,

the values of temperature increase were calculated for the values of averaged powers, which are obtained by interpolation curve. Results achieved by calculation and measurement are shown in **Table 4**. The differences between the calculated and measured values are within 1÷16%.

**Table 3** The results of calculation

Parameter	Value	Unit	Description
$\rho$	7522	kg/m <sup>3</sup>	density of the round
$a$	$5.4 \cdot 10^{-6}$	m <sup>2</sup> /s	coefficient of thermal diffusivity of the round
$\alpha$	164.43	W/m <sup>2</sup> K	overall heat transfer coefficient
$ Fo $	0.01492		Fourier number
$ Bi $	0.7938		Biot number
$\psi$	0.8344		factor of massiveness of the body
$\Phi_0$	205.6	kW	heat flow from the body to the environment
$\Phi$	1205.8	kW	transformed mechanical energy to internal energy
$\vartheta_{out,cal.}$	1180	°C	calculated output temperature
$\vartheta_{out,exp}$	1190	°C	measured output temperature

**Table 4** The experimental and calculated data

$\vartheta_{in,exp} / ^\circ\text{C}$	1050	1080	1100	1125	1152	1180	1210	1250
$\vartheta_{out,exp} / ^\circ\text{C}$	1172	1190	1192	1201	1217	1224	1248	1280
$\Delta\vartheta_{exp} / ^\circ\text{C}$	122	110	92	76	65	44	38	30
$P_{exp} / \text{MW}$	1.489	1.391	1.218	1.070	0.976	0.773	0.735	0.685
$\Delta\vartheta_{cal} / ^\circ\text{C}$	124.6	103.3	90.8	76.8	63.5	51.2	39.6	26.1

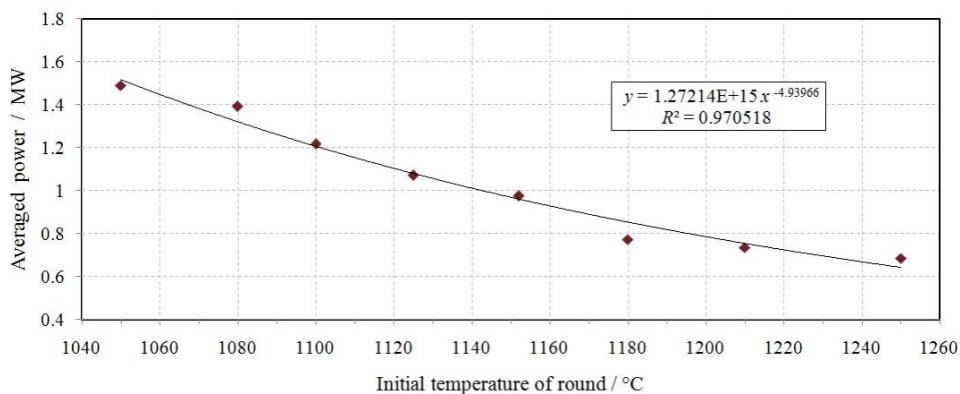


**Fig. 5** Electric motor power in relation to the initial temperature of the round

## Conclusions

The article presents formulated mathematical model for calculating the temperature increase of the the tick-walled hollow shell, during the cross roll piercing operation, depending on the initial temperature of the round as well as the electric energy consumed for drive of the work rolls. On the basis of the measured essential parameters, the formulated mathematical model for energy transformations during the piercing process was validated.

The purpose of the model is for a certain format and chemical composition of the round, taking into account the necessary initial rolling temperature in the next pilger process, to determine the optimum round temperature on the exit of the furnace. By lowering the stock output temperature the significant savings in fuel consumption of rotary hearth furnace could be achieved. In the process of optimizing the energy consumption in line for the production of seamless tubes, it is necessary to consider that lowering the initial round temperature in the cross roll piercing process causes an increase in the consumption of electric energy for drive of the rollers as well as an increased wear of rolls.

## References

- [1] V. L. Brovkin et al.: Acta Metallurgica Slovaca, Vol. 20, 2014, No. 4, p. 381-388, doi:10.12776/ams.v20i4.388
- [2] L. Lazić, V. Brovkin, A. Varga, J. Kizek: Acta Metallurgica Slovaca Conference, Vol. 2, 2011, No. 1, p. 118-125
- [3] L. Lazić, V. Brovkin, A. Varga, J.Kizek: Acta Metallurgica Slovaca Conference, Vol. 15, 2009, No. 1, p. 159-167
- [4] Y.N. Radachenko, L.V. Brovkin, S. I. Reshetnyak, L. Lazić, A. Varga, J. Kizek: Acta Metallurgica Slovaca Conference, Vol. 2, 2011, No. 1, p. 176-183
- [5] J. Črnko, P. Jelić, L. Lazić, M. Kundak: Metalurgija, Vol. 46, 2007, No. 4, p. 291-293
- [6] J. Črnko, P. Jelić, M. Kundak, L. Lazić: Metalurgija, Vol. 47, 2008, No. 2, p. 139-141
- [7] L. Lazić, P. Jelić, J. Črnko, V. L. Brovkin: Acta Mechanica Slovaca, Vol. 4-D, 2007, p. 103-108
- [8] L. Lazić, Ž. Grubišić, M. Lovrenic-Jugovic: Acta Metallurgica Slovaca, Vol. 20, 2014, No. 2, p. 244-251, doi:10.12776/ams.v20i1.299
- [9] K. H. Brensing, K. H. Sommer: *Steel tube and pipe manufacturing processes*, [25.10.2014] [http://www.smrw.de/files/steel\\_tube\\_and\\_pipe.pdf](http://www.smrw.de/files/steel_tube_and_pipe.pdf)
- [10] K. Komori, K. Mizuno: Journal of Materials Processing Technology, Vol. 209, 2009, No. 11, p. 4994–5001, doi:10.1016/j.jmatprotec.2009.01.022
- [11] K. Komori: International Journal of Mechanical Science, Vol. 47, 2005, No. 12, p. 1838–1853, doi:10.1016/j.ijmecsci.2005.07.009
- [12] D. A. Berazategui, M. A. Cavaliere, L. Montelatici, E. N. Dvorkin: International Journal for Numerical Methods in Engineering, Vol. 65, 2006, No. 7, p. 1113–1144, doi:10.1002/nme.1475
- [13] K. Komori, M. Suzuki: Journal of Materials Processing Technology, Vol. 169, 2005, p. 249–257, doi:10.1016/j.jmatprotec.2005.03.017
- [14] W. Kubinski, J. Kazanecki, J. Starowicz: Journal of Materials Processing Technology, Vol. 34, 1992, No. 1-4, p. 333–339
- [15] E. Erman: Journal of Mechanical Working Technology, Vol. 15, 1987, No. 2, p.167–179
- [16] N. Yu. Tayts: *Tekhnologiya nagreva stali (Steel Heating Technology)*, Metallurgizdat, Moskva, 1962
- [17] V. Krivandin, B. Markov: *Metallurgical Furnaces*, MIR Publishers, Moscow, 1977
- [18] M. N. Ozisik: *Heat Transfer – A Basic Approach*, McGraw-HillInternational, 1984